

The GGCMI Phase II experiment: global gridded crop model simulations under uniform changes in CO₂, temperature, water, and nitrogen levels (protocol version 1.0)

James Franke^{1,2}, Christoph Müller³, Joshua Elliott^{2,4}, Alex C. Ruane⁵, Abigail Snyder⁶, Jonas Jägermeyr^{3,2,4,5}, Juraj Balkovic^{7,8}, Philippe Ciais^{9,10}, Marie Dury¹¹, Pete Falloon¹², Christian Folberth⁷, Louis François¹¹, Tobias Hank¹³, Munir Hoffmann^{14,23}, R. Cesar Izaurralde^{15,16}, Ingrid Jacquemin¹¹, Curtis Jones¹⁵, Nikolay Khabarov⁷, Marian Koch¹⁴, Michelle Li^{2,17}, Wenfeng Liu^{9,18}, Stefan Olin¹⁹, Meridell Phillips^{5,20}, Thomas A. M. Pugh^{21,22}, Ashwan Reddy¹⁵, Xuhui Wang^{9,10}, Karina Williams¹², Florian Zabel¹³, and Elisabeth Moyer^{1,2}

¹Department of the Geophysical Sciences, University of Chicago, Chicago, IL, USA

²Center for Robust Decision-making on Climate and Energy Policy (RDCEP), University of Chicago, Chicago, IL, USA

³Potsdam Institute for Climate Impact Research, Member of the Leibniz Association, Potsdam, Germany

⁴Department of Computer Science, University of Chicago, Chicago, IL, USA

⁵NASA Goddard Institute for Space Studies, New York, NY, United States

⁶Joint Global Change Research Institute, Pacific Northwest National Laboratory, College Park, MD, USA

⁷Ecosystem Services and Management Program, International Institute for Applied Systems Analysis, Laxenburg, Austria

⁸Department of Soil Science, Faculty of Natural Sciences, Comenius University in Bratislava, Bratislava, Slovak Republic

⁹Laboratoire des Sciences du Climat et de l'Environnement, CEA-CNRS-UVSQ, 91191 Gif-sur-Yvette, France

¹⁰Sino-French Institute of Earth System Sciences, College of Urban and Env. Sciences, Peking University, Beijing, China

¹¹Unité de Modélisation du Climat et des Cycles Biogéochimiques, UR SPHERES, Institut d'Astrophysique et de Géophysique, University of Liège, Belgium

¹²Met Office Hadley Centre, Exeter, United Kingdom

¹³Department of Geography, Ludwig-Maximilians-Universität, Munich, Germany

¹⁴Georg-August-University Göttingen, Tropical Plant Production and Agricultural Systems Modeling, Göttingen, Germany

¹⁵Department of Geographical Sciences, University of Maryland, College Park, MD, USA

¹⁶Texas AgriLife Research and Extension, Texas A&M University, Temple, TX, USA

¹⁷Department of Statistics, University of Chicago, Chicago, IL, USA

¹⁸EAWAG, Swiss Federal Institute of Aquatic Science and Technology, Dübendorf, Switzerland

¹⁹Department of Physical Geography and Ecosystem Science, Lund University, Lund, Sweden

²⁰Earth Institute Center for Climate Systems Research, Columbia University, New York, NY, USA

²¹School of Geography, Earth and Environmental Sciences, University of Birmingham, Birmingham, UK.

²²Birmingham Institute of Forest Research, University of Birmingham, Birmingham, UK.

²³Leibniz Centre for Agricultural Landscape Research (ZALF), D-15374 Müncheberg, Germany

Correspondence: Christoph Müller (cmueller@pik-potsdam.de)

Abstract. Concerns about food security under climate change motivate efforts to better understand future changes in crop yields. Process-based crop models, which represent plant physiological processes, are necessary tools for this purpose since they allow representing future climate and management conditions not sampled in the historical record and new locations where cultivation may shift. However, models remain uncertain and differ in many critical details. The Global Gridded Crop Model Intercomparison (GGCMI) Phase II experiment, an activity of the Agricultural Model Intercomparison and Improve-

ment Project (AgMIP), is designed to allow systematic evaluation and “emulation” of model responses to multiple interacting factors. In this paper we describe the GGCMI Phase II experimental protocol (simulations run with systematic uniform perturbations of historical climate) and its simulation data archive (from twelve crop models and five crops). We also present different model outputs in different aggregations across the CTNW space in order to illustrate the data richness of the GGCMI

5 Phase II archive and to discuss some general characteristics of the simulation data set. Modeled yields show robust decreases to warmer mean climatologies in almost all regions, with a nonlinear dependence that means yield changes in warmer baseline locations are more sensitive to temperature increases. Inter-model uncertainty is qualitatively similar across all the four input dimensions, but is highest in high-latitude regions where crops may be grown in the future.

1 Introduction

10 Understanding crop yield response to a changing climate is critically important, especially as the global food production system will face pressure from increased demand over the next century (Bodirsky et al., 2015). Climate-related reductions in supply could therefore have severe socioeconomic consequences (e.g. Stevanović et al., 2016; Wiebe et al., 2015). Multiple studies using different crop or climate models concur in projecting sharp yield reductions on currently cultivated cropland under business-as-usual climate scenarios, although their yield projections show considerable spread (e.g. Rosenzweig et al., 2014;

15 Schauberger et al., 2017; Porter et al. (IPCC), 2014, and references therein). Modeling crop responses continues to be challenging, as crop growth is a function of complex interactions between climate inputs and management practices (J. Boote et al., 2013; Rötter et al., 2011). Intercomparison projects such as the Agricultural Model Intercomparison and Improvement Project (AgMIP Rosenzweig et al., 2013) have helped to quantify uncertainties in model projections (Rosenzweig et al., 2014), developed protocols (Elliott et al., 2015) for evaluating model performance (Müller et al., 2017) and analyzed selected mechanisms

20 (e.g. Schauberger et al., 2017). Models tend to agree broadly in major response patterns, including a reasonable representation of the spatial pattern in historical yields of major crops (e.g. Elliott et al., 2015; Müller et al., 2017) and projections of shifts in yield under future climate scenarios.

25 Process-based crop models are a family of numerical models that simulate the process of photosynthesis and the biology and phenology of individual crops. Process-based crop models provide some advantages over statistical crop models when used for climate change assessments. The ability to incorporate direct fertilization from atmospheric CO₂ Globally-gridded crop models allow flexibility in spatial assessment .. and to study future cultivation area changes and crop selection switching under climate change.

30 Process-based models still struggle with some important details, including reproducing historical year-to-year variability in various countries (e.g. Müller et al., 2017), reproducing historical yields when driven by reanalysis weather (e.g. Glotter et al., 2014), and low sensitivity to extreme events (e.g. Glotter et al., 2015; Jägermeyr and Frieler, 2018; Schewe et al., 2019). These issues are driven in part by the diversity of new cultivars and genetic variants, which outstrips the ability of academic modeling groups to capture them (e.g. Jones et al., 2017). Models also do not simulate many additional factors affecting production, including but not limited to: pests, diseases, and weeds. For these reasons, individual studies must generally re-

calibrate models to ensure that short-term predictions reflect current cultivars and management levels, and long-term projections retain considerable uncertainty (Wolf and Oijen, 2002; Jagtap and Jones, 2002; Iizumi et al., 2010; Angulo et al., 2013; Asseng et al., 2013, 2015). Inter-model discrepancies can also be high in areas not yet cultivated (e.g. Challinor et al., 2014; White et al., 2011). Finally, process-based models present additional difficulties for high-resolution global studies because of their complexity and computational requirements, as well as the general inability to calibrate site-specific parameters.

Nevertheless, process-based models are necessary for understanding the future yield impacts of climate change as well as options for climate mitigation (Müller et al., 2015) and adaptation (Challinor et al., 2018), future sustainable development (Humpenöder et al., 2018), and food security (Wheeler and Von Braun, 2013). Despite the additional uncertainty and challenges to run crop models at the global scale (Müller et al., 2017), gridded, global crop model applications are much needed for consistent assessments. Climate change and international agricultural trade often require to consider the global and local dynamics (Rosenzweig et al., 2018; Ruane et al., 2018) and global market mechanisms may strongly modulate climate change impacts (Stevanović et al., 2016; Hasegawa et al., 2018). Cultivation may shift to new areas, where no yield data are currently available and therefore statistical models cannot be applied. Finally, only process-based models can capture the growth response to novel conditions and practices that are not represented in historical data (e.g. Pugh et al., 2016; Roberts et al., 2017). These novel changes can include the direct fertilization effect of elevated CO₂, and changes in management practices that may mitigate climate-induced damages (e.g. Minoli et al., 2019).

Understanding process-based models' responses to important drivers are thus critical to improve future projections of agricultural productivity. The Global Gridded Crop Model Intercomparison (GGCMI) of AgMIP (Elliott et al., 2015) has thus designed a 2nd phase (*Phase II*) with a focus on models' response to changes in the most important model drivers: atmospheric carbon dioxide concentrations ([CO₂], C), temperature (T), water (W), and nitrogen (N). The CTWN experiment is inspired by AgMIP's Coordinated Climate-Crop Modeling Project (C3MP Ruane et al., 2014; McDermid et al., 2015) and has been extended by the nitrogen dimension and contributes to the AgMIP Coordinated Global and Regional Assessments (CGRA) (Ruane et al., 2018; Rosenzweig et al., 2018). To account for the importance of adaptation in agricultural production to climate change, a fifth dimension, adaptation (A) has been added to the CTWN experiment. The A dimension only has two elements, namely *no adaptation* and one *adaptation* setting, in which the growing season that is shortened under warming, is regained by adapted crop cultivar choice.

In this paper, we describe the GGCMI Phase II model experiments and present initial summary results.
The following sections provide the goals and protocols
models included and at what levels of participation
30 Simulation assessment is provided with comparison to FAO yield data at the country level
Finally we show some selected slices of the simulation output dataset to illustrate spread in model response across some of the input dimension

2 Simulation objectives, protocol, and models

2.1 Goals

35 GGCMI Phase II is the continuation of a multi-model comparison exercise begun in 2014. The initial Phase I compared harmonized yield simulations of 21 models for 19 crops over the historical period with a primary goal of model evaluation (Elliott et al., 2015; Müller et al., 2017) and understanding of different sources of uncertainty, such as model parameterization (Folberth et al., 2016), different weather products, or aggregation (Porwollik et al., 2017). Phase II compares simulations of 12 models for 5 crops (maize, rice, soybean, spring wheat, and winter wheat) using only one of the weather products used
5 in Phase I, which was then perturbed systematically for the different simulations. The reduced set of crops includes the three major global cereals and the major legume and accounts for over 50% of human calories (in 2016, nearly 3.5 billion tons or 32% of total global crop production by weight (Food and Agriculture Organization of the United Nations, 2018), which were also in the focus of analyses in the previous analyses (Elliott et al., 2015; Müller et al., 2017; Porwollik et al., 2017) and for which global sub-national reference data exist (Ray et al., 2012; Iizumi et al., 2014).

10 The guiding scientific rationale of GGCMI Phase II is to provide a comprehensive, systematic evaluation of the response of process-based crop models to [CO₂], temperature, water, and applied nitrogen (collectively referred to as “CTWN”). Given that the production of annual crops is continuously changing by making use of new varieties and technologies (Olesen et al., 2012) it is plausible to assume at least some degree of adaptation to new climate conditions. We thus also include one additional simulation set across the entire CTWN space with just one simple adaptation setting (A), in which we assume that varieties
15 are grown at each temperature level, that maintain the growing season, i.e. that reach maturity at the same time as current varieties under current temperature regimes. We acknowledge that this is an overly simplistic assumption that does not reflect the range of opportunities and limitations to adaptation (Vadez et al., 2012; Challinor et al., 2018). Still, this setting allows to demonstrate the role of adaptation and is easy to integrate into the modeling protocol as growing seasons have to be harmonized across groups anyway. The dataset is designed to allow researchers to:

- 20 – Enhance understanding of how models work by characterizing their sensitivity to input climate and nitrogen drivers.
- Study the interactions between climate variables and nitrogen inputs in driving modeled yield impacts.
- Explore differences in crop response to warming across the Earth’s climate regions.
- Provide a dataset that allows statistical emulation of crop model responses for downstream modelers.
- Illustrate differences in potential adaptation via growing season changes.

25 2.2 Modeling protocol

The phase II protocol focuses on climatological perturbations from historical weather in the period 1980-2010 at different management and atmospheric CO₂ levels. The experimental protocol consists of 9 levels for precipitation perturbations, 7 for

temperature, 4 for $[CO_2]$, and 3 for applied nitrogen, for a total of 672 simulations for rainfed agriculture and an additional 84 for irrigated (Table 1). For irrigated simulations, limitations from actual water supply are not considered. Limits for the climate
30 variable perturbations are selected to represent reasonable ranges for potential climate changes in the medium term. Note that $[CO_2]$ changes are applied independently of changes in climate variables, so that higher $[CO_2]$ is not associated with higher temperatures. The resulting GGCMI Phase II dataset captures a distribution of crop responses over the potential space of future climate conditions.

Each model is run at 0.5 degree spatial resolution and covers all currently cultivated areas and much of the uncultivated land area. (See Figure 1 for the present-day cultivated area of rainfed crops, and Figure S1 in the Supplemental Material for irrigated crops.) To reduce the computational burden, we provide a boolean mask, identifying regions that are unsuitable
5 for cropland for non-climatic reasons. For this, we use a combination of soil suitability indices at 10 arc minute resolution for excess salt, oxygen availability, rooting conditions, toxicities, and workability according to GAEZ (?) (downloaded from www.gaez.iiasa.ac.at/), following the procedure as proposed by Pugh et al. (2016). We excluded all 0.5 arc degree grid cells in which at least 90% of the area was masked as unsuitable — i.e. not categorized as "minimal" or "moderate" constraints according to any of these suitability indices. There are a few cases, where (at the resolution of 0.5 degrees) the grid cell is
10 classified as dominantly unsuitable but the cropland masks assign cropland to these grid cells. To ensure that all cropland currently used in the aggregation is also simulated by the groups, we exclude only pixels that are predominantly unsuitable ($\geq 90\%$) and do not contain any cropland (according to MIRCA2000 (Portmann et al., 2010)).

Coverage extends considerably outside currently cultivated areas because cultivation will likely shift under climate change. However, areas are not simulated in some cases if they are assumed to remain non-arable even under an extreme climate
15 change; these regions include Greenland, far-northern Canada, Siberia, Antarctica, the Gobi and Sahara Deserts, and central Australia. All models produce as output crop yields (tons $ha^{-1} year^{-1}$) for each 0.5 degree grid cell. For illustration purposes here, we take as the baseline the scenario with historical climatology (i.e. T and P changes of 0), C of 360 ppm, and applied N at 200 kg N ha^{-1} . This must not be confused with a correct historic setup, as there is no trend in the $[CO_2]$ and the uniform application of 200 kg N ha^{-1} is not representative for many world regions (Elliott et al., 2015). The GGCMI Phase
20 II simulations are designed for evaluating changes in yield across the CTNW-A space but not necessarily absolute yields, since they omit detailed calibrations. To provide some evaluation of the skill of the process-based models used, we repeat the evaluation exercises of Müller et al. (2017) for GGCMI Phase I but stress that in particular the uniform fertilizer application does not represent the actual situation.

2.2.1 Input data and harmonization

In most cases, historical daily climate inputs are taken from the 0.5 degree NASA AgMERRA daily gridded re-analysis product specifically designed for agricultural modeling, with satellite-corrected precipitation (Ruane et al., 2015), but two models (JULES and PROMET) require sub-daily input data and use their own alternative baseline climate inputs (WFDEI (Weedon et al., 2014) and ERA-Interim (Dee et al., 2011), respectively).

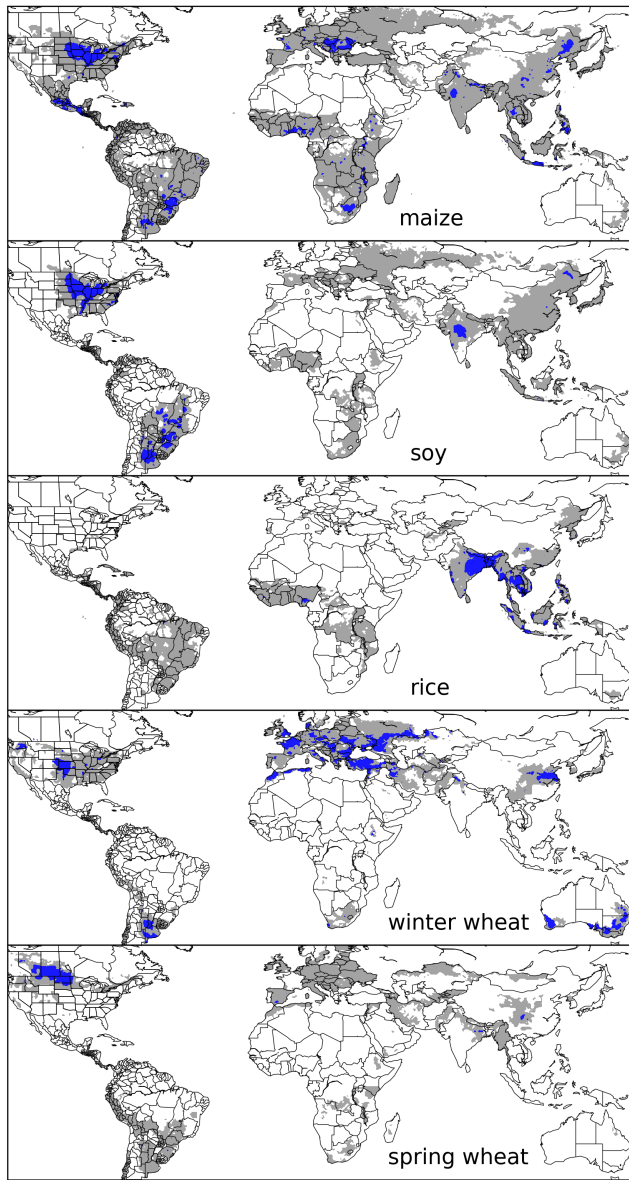


Figure 1. Presently cultivated area for rainfed crops. Blue indicates grid cells with more than 20,000 hectares ($\sim 10\%$ of an equatorial grid cell). Gray contour shows area with more than 10 hectares cultivated. Cultivated areas for maize, rice, and soybean are taken from the MIRCA2000 (“monthly irrigated and rainfed crop areas around the year 2000”) dataset (Portmann et al., 2010). Areas for winter and spring wheat areas are adapted from MIRCA2000 data and sorted by growing period. For analogous figure of irrigated crops, see Figure S1.

Temperature perturbations are applied as absolute offsets from the daily mean, minimum, and maximum temperature time series for each grid cell. Precipitation perturbations are applied as fractional changes at the grid cell level, and $[CO_2]$ and

Table 1. GGCMI Phase II input levels. Temperature and precipitation values indicate the perturbations from the historical climatology. W- percentage does not apply to the irrigated (W_{inf}) simulations, which are all simulated at the maximum beneficial levels of water. Bold font indicates the ‘baseline’ historical level. One model provided simulations at the T + 5 level. See Figure S3 in the supplement for number of simulations associated with each combination of input levels.

Input variable	Tested range	Unit
[CO ₂] (C)	360 , 510, 660, 810	ppm
Temperature (T)	-1, 0 , 1, 2, 3, 4, 6	°C
Precipitation (W)	-50, -30, -20, -10, 0 , 10, 20, 30, (and W_{inf})	%
Applied nitrogen (N)	10, 60, 200	kg ha ⁻¹
Adaptation (A)	A0: none , A1: new cultivar to maintain original growing season length	-

nitrogen levels are specified as discrete values applied uniformly over all grid cells. No other N inputs are assumed (i.e. no atmospheric deposition), but soil mineralization can supply additional plant-available N, which can vary by model.

Growing seasons are standardized across models (with assumptions based on Sacks et al. (2010) and Portmann et al. (2008, 2010)), but vary by crop and by location on the globe. For example, maize is sown in March in Spain, in July in Indonesia, and in December in Namibia. Only growing seasons for rainfed systems are used in GGCMI Phase II, as full irrigation is treated as one perturbation level in the W dimension (“Winf”). Growing seasons for maize, rice, and soybean have been used from Phase I (Elliott et al., 2015), but wheat was separated into spring wheat (swh) and winter wheat (wwh) so that new growing season data had to be provided. For this, wheat crop calendars were separated following simple rules. The SAGE crop calendar 5 (Sacks et al., 2010) provides separate spring and winter cropping seasons. This was used as primary source of information, as for the other crops (Elliott et al., 2015). In areas, where no SAGE crop calendar information is available, the MIRCA2000 crop calendar (Portmann et al., 2010) was used. Wheat growing seasons were assigned to winter wheat if

- the mean monthly temperature is below freezing point (<0°C) at most for 5 months per year,
- the coldest 3 months of a year are below 10°C
- 10 – the season starts after the warmest or before the coldest month of the year on the northern hemisphere, or
- the season starts after the warmest and before the coldest month of the year on the southern hemisphere

and were assigned to spring wheat otherwise. For areas where also not MIRCA2000 crop calendar was available, simulated LPJmL growing seasons (Waha et al., 2012) were used as in Phase I (Elliott et al., 2015), applying the same rules as for MIRCA2000 to distinguish spring wheat from winter wheat seasons.

15 As per convention, N fertilizer is to be applied in two doses to reduce losses to the environment. For simplicity, the first half of the total fertilizer input is to be applied at sowing and the other half is to be applied on day 40 after sowing for all crops except for winter wheat. For winter wheat, the application date for the second N fertilizer application was provided, because the length of dormancy during winter can be quite variable across regions. The second fertilization date for winter wheat was set to the middle day of the first month with average temperatures above 5°C after sowing with a minimum distance to the maturity date of 50 days and to planting of 40 days.

All stresses are disabled other than factors related to nitrogen, temperature, and water (e.g. alkalinity, salinity, non-nitrogen nutrients). No additional nitrogen inputs, such as atmospheric deposition, are considered, but some model treatments of soil
5 organic matter allows additional nitrogen release through mineralization.

2.2.2 Output data conventions and file names

All output data is supplied as netCDF version 4 files as in GGCM Phase I (Elliott et al., 2015) following a similar naming convention. As the ISIMIP file naming convention now includes the identifier *global* to distinguish regional from global model output (Frieler et al., 2017), we follow that convention here as well:

10 [model]_[climate]_hist_fullharm_[irrig.scenario]_[variable]_[crop]_global_annual_[start-year]_[end-year].nc4
where [model] is the GGCM name, [climate] is the original climate input data set (typically AgMERRA), [irrig.scenario] is the irrigation setting ("fир" for fully irrigated and "noir" for fully rainfed), [variable] is the output variable (see Table 2), [crop] is the crop abbreviation ("mai" for maize, "ric" for rice, "soy" for soybean, "swh" for spring wheat, "wwh" for winter wheat), [start - year]_[end - year] specify the first and last year recorded on file. The entire file name needs to be in small
15 caps. The first entry in the file is the result of the first simulated cropping cycle that is entirely within the given climate input. For AgMERRA, where the first year provided is 1980, the first harvest record is thus of 1980, when the prescribed sowing and harvest dates are in 1980 (e.g. sowing in March and harvest in September 1980) but is of 1981 if sowing is later in a calendar year than harvest (e.g. sowing in September 1980 and harvest in March 1981). To avoid distortions in harvest events, output
20 files report the sequence of growing periods rather than calendar years. In most cases, this is equivalent, as there is always only one sowing event per calendar year. As harvest events are internally determined as a function of mostly temperature, these can vary between individual years. If harvest events are around the end of the calendar year (Dec. 31), reported values could contain
2 2 (one in early January and one in late December), 1 (normal) or none (last was in December of previous year and next is in January of the following year) harvest event if reported per calendar year. As in Phase I, all output data need to be provided
25 on a regular geographic grid, spanning latitudes from -89.75 to 89.75° and longitudes from -179.75 to 179.75° (referring to the center of each grid cell). Missing values, i.e. where no crop growth has been simulated, such as ocean grid cells, need to be reported as 1.e+20f whereas crop failure should be reported as zero yield. Following NetCDF standards, latitude, longitude and time must be included as separate variables in ascending order. Units of these axes are "degrees north", "degrees east", and
"growing seasons since YYYY-01-01 00:00:00", where YYYY indicates the first year (1980 for AgMERRA).

Next to simulated yield data, crop modelers are requested to provide additional output variables (Table 2).

Table 2. Main output variables requested per crop. Mandatory outputs (if available in that GGCM) in **bold**. Some models provide additional variables, such as more detailed separation of total nitrogen losses.

Variable	variable name	units
Yield	yield_<crop>	t ha⁻¹ yr⁻¹ (dry matter)
Total above ground biomass yield	biom_<crop>	t ha⁻¹ yr⁻¹ (dry matter)
Actual planting date	plant-day_<crop>	day of year
Anthesis date	anth-day_<crop>	days from planting
Maturity date	maty-day_<crop>	days from planting
Applied irrigation water	pirrww_<crop>	mm yr⁻¹
Evapotranspiration (growing season sum)	etransp_<crop>	mm yr⁻¹ (firr scenarios only)
Transpiration (growing season sum)	transp_<crop>	mm yr ⁻¹
Evaporation (growing season sum)	evap_<crop>	mm yr ⁻¹
Runoff (total growing season sum, subsurface + surface)	runoff_<crop>	mm yr ⁻¹
Total available soil moisture in root zone *	trzpah2o_<crop>	mm yr ⁻¹
Total root biomass	rootm_<crop>	t ha ⁻¹ yr ⁻¹ (dry matter)
Total Nr uptake (total growing season sum)	tnrup_<crop>	kg ha ⁻¹ yr ⁻¹
Total Nr inputs (total growing season sum)	t nrin_<crop>	kg ha ⁻¹ yr ⁻¹
Total Nr losses (total growing season sum)	t nrloss_<crop>	kg ha ⁻¹ yr ⁻¹
Gross primary production (GPP)	gpp_<crop>	gC m ⁻² yr ⁻¹
Net primary production (NPP)	npp_<crop>	gC m ⁻² yr ⁻¹
CO ₂ response scaler on NPP	co2npp_<crop>	- {0..inf}
water response scaler on NPP	h2onpp_<crop>	- {0..1}
temperature response scaler on NPP	tnpp_<crop>	- {0..1}
Nr response scaler on NPP	n rnpp_<crop>	- {0..1}
Other nutrient response scaler on NPP	ornpp_<crop>	- {0..1}
CO ₂ response scaler on transpiration	co2trans_<crop>	- {0..1}
maximum stress response scaler	maxstress_<crop>	- {0..1}
Maximum LAI	laimax_<crop>	m ² m ⁻²

* growing season sum, basis for computing average soil moisture

30 A script for initial data quality screening has been provided to the modeling groups so that these could test plausible data range and spatial coverage prior to data submission.

2.3 Models contributing

The protocol described above has been implemented by 12 GGCMs which have supplied data to the GGCMI Phase II archive. Given the substantial computational requirements for participation in GGCMI Phase II with 756 (A0) + 648 (A1) global 31-year simulations for 5 different crops, we specified different participation tiers to allow submission of smaller sub-sets. These subsets were designed as orthogonal samples across the 4 dimensions of the CTWN space. These are designed by combinations of selected pairs in the CxN space (all 12 vs. 4 pairs: C360_N10, C360_N200, C660_N60, C810_N200) and the TxW space:

5 sa *minimum set* with an orthogonal, stratified 9-step sampling (T-1W-10, T0W10, T1W-30, T2W-50, T2W20, T3W30, T4W0, T4Winf, T6W-20) a *reduced set* of alternating combinations, which uses different W for even Ts than for odd Ts. For even Ts (i.e. T0,T2,T4,T6), we use $W = -50,-20,0,+30 = 4^*4$, for odd Ts (i.e. T-1,T1,T3), we use $W = -30, -10, +10, +30, \text{inf} = 3^*5$, and the *full set* (all 7Tx9W)

The different participation levels are thus defined by combining the CxN sets with the TxW sets:

- 10 – **full**: all 756 (648) A0 (A1) simulations (all 12 CxN * all 63 TxW)
- **high tier**: 362 simulations (all 12 CxN combinations * *reduced* TxW set of 31 combinations)
- **mid tier**: 124 simulations (low 4 CxN combinations * *reduced* TxW set of 31 combinations)
- **low tier**: 36 simulations (low 4 CxN combinations * *minimum* TxW set of 9 combinations)

The 12 models included in GGCMI Phase II are all process-based crop models that are widely used in impacts assessments
15 (Table 3). Although some models share a common base (e.g. the LPJ family or the EPIC family of models), they have subsequently developed independently. Differences in model structure mean that several key factors are not standardized across the experiment, such as carry-over effects across growing years including residue management and soil moisture, and the extent of simulated area for different crops. Not all modeling teams provide the full simulation protocol, for instance, CARIAB and JULES do not simulate the nitrogen dimension and some crops are not parameterized in each model (see Table 3 for details).

20 3 Results

We provide some comparison of model results to FAO data records to describe the models' skill in reproducing crop yield characteristics. We stress that the comparison is not straightforward as none of the settings in the CTWN-A experiment design reflects actual conditions. For a more rigorous evaluation of the models' performance, we refer to the GGCMI model evaluation study of Müller et al. (2017). In order to illustrate the data structure and general features of the ensemble, we show selected
25 results in different aggregation levels (maps, regional aggregations). We focus on yield data, as this dataset if presumably of greatest interest and yield data are the more important and best evaluated outputs of GGCMs.

Table 3. Models included in GGCMI Phase II and the number of C, T, W, and N simulations that each performs, with 756 as the maximum for A0 (no adaptation) and 648 as the maximum for A1 (maintaining growing season adaptation). “N-Dim.” indicates whether the simulations include varying nitrogen levels. Two models provide only one nitrogen level. All models provide the same set of simulations across all modeled crops, but some omit individual crops. (For example, APSIM does not simulate winter wheat.)

Model (Key Citations)	Maize	Soybean	Rice	Winter wheat	Spring wheat	N dim.	Sims per crop (A0 / A1)
APSIM-UGOE , Keating et al. (2003); Holzworth et al. (2014)	X	X	X	–	X	X	44 / 36
CARAIB , Dury et al. (2011); Pirttioja et al. (2015)	X	X	X	X	X	–	252 / 216
EPIC-IIASA , Balkovič et al. (2014)	X	X	X	X	X	X	39 / 0
EPIC-TAMU , Izaurralde et al. (2006)	X	X	X	X	X	X	765 / 648
JULES , Osborne et al. (2015); Williams and Falloon (2015); Williams et al. (2017)	X	X	X	–	X	–	252 / 0
GEPIC , Liu et al. (2007); Folberth et al. (2012)	X	X	X	X	X	X	430 / 181
LPJ-GUESS , Lindeskog et al. (2013); Olin et al. (2015)	X	–	–	X	X	X	756 / 648
LPJmL , von Bloh et al. (2018)	X	X	X	X	X	X	756 / 648
ORCHIDEE-crop , Wu et al. (2016)	X	–	X	X	–	X	33 / 0
pDSSAT , Elliott et al. (2014); Jones et al. (2003)	X	X	X	X	X	X	756 / 648
PEPIC , Liu et al. (2016a, b)	X	X	X	X	X	X	149 / 121
PROMET , Hank et al. (2015); Mauser et al. (2015)	X	X	X	X	X	X	261 / 232
Totals	12	10	11	11	11	10	5240 / 3378

3.1 Simulation Assessment

The Müller et al. (2017) procedure evaluates response to year-to-year temperature and precipitation variations in a control run driven by historical climate and compares it to detrended historical yields from the FAO (Food and Agriculture Organization of the United Nations, 2018) by calculating the Pearson product moment correlation coefficient. The procedure is sensitive

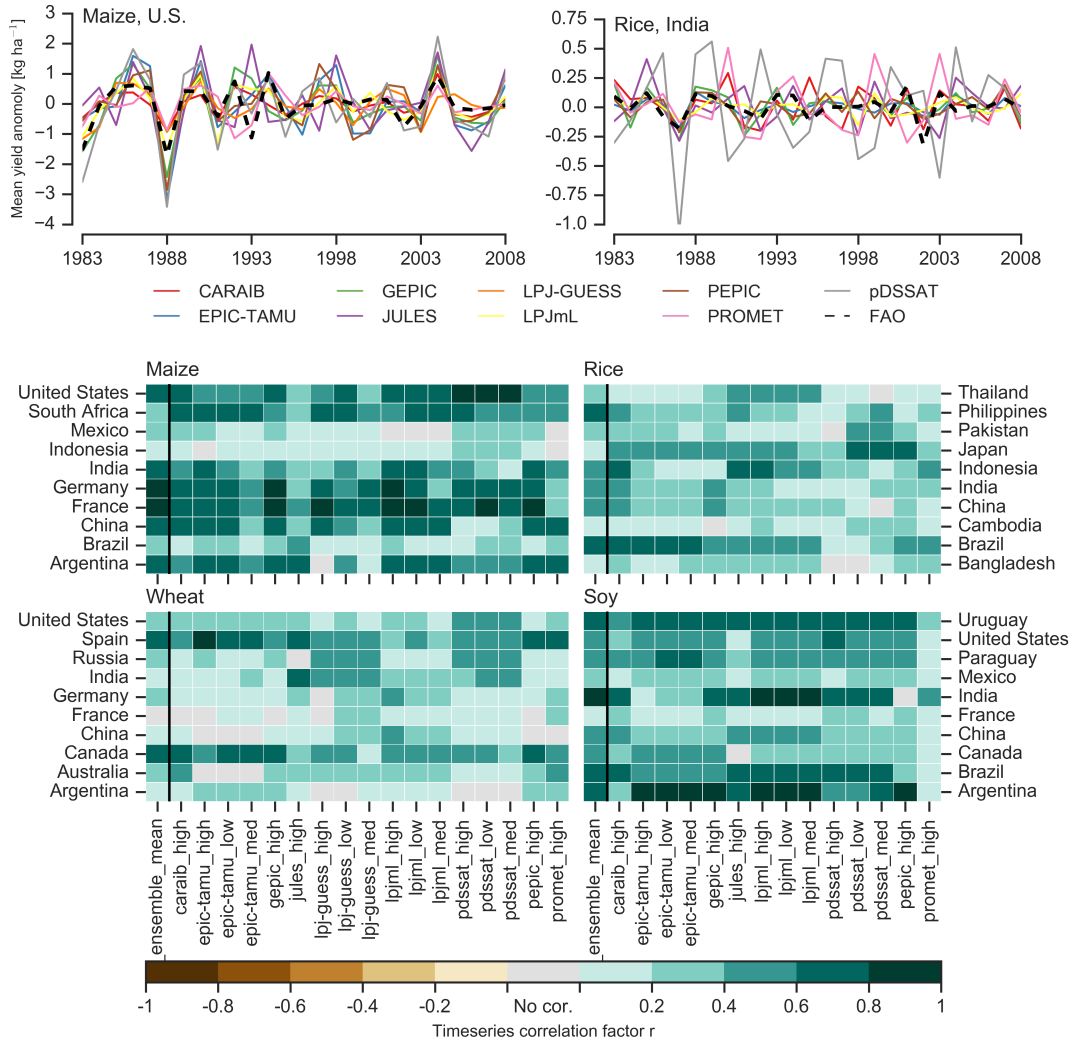


Figure 2. Time series of correlation coefficients between simulated crop yield and FAO data (Food and Agriculture Organization of the United Nations, 2018) at the country level. The top panels indicate two example cases: US maize (a good case), and rice in India (mixed case), both for the high nitrogen application case. The heatmaps illustrate the Pearson r correlation coefficient between the detrended simulation mean yield at the country level compared to the detrended FAO yield data for the top producing countries for each crop with continuous FAO data over the 1981-2010 period. Models that provided different nitrogen application levels are shown with low (10 kg N ha^{-1}), med (60 kg N ha^{-1}), and high (200 kg N ha^{-1}) label (models that did not simulate different nitrogen levels are analogous to a high nitrogen application level). The ensemble mean yield, show in the leftmost column, is also correlated with the FAO data (not the mean of the correlations). Wheat contains both spring wheat and winter wheat simulations where supplied, else one or the other (see Table 3). The Pearson r correlation coefficients are similar to those of GGCMI Phase I, with reasonable fidelity at capturing year-over-year variation, with differences by region and crop stronger than difference between models as indicated by more horizontal bars than vertical bars of the same color.

to the detrending method and the area mask used to aggregate yields. Here we use a 5-year running mean removal and the MICRA area mask for aggregation. In some cases the time series are shifted by one year to account for errors in FAO or model year reporting. The procedure offers no means of assessing CO₂ fertilization, since [CO₂] has been relatively constant over the historical data collection period. Nitrogen introduces another source of uncertainty into the analysis, since the GGCMI Phase II runs impose fixed, uniform nitrogen application levels that are not realistic for individual countries. We evaluate up to three control runs for each model, since some modeling groups provide historical runs for three different nitrogen levels.

5 Results are similar to those of GGCMI Phase I, with reasonable fidelity at capturing year-over-year variation, with differences by region and crop stronger than difference between models. (That is, Figure 2 shows more similarity in horizontal than vertical bars.) No single model is dominant, with each model providing near best-in-class performance in at least one location-crop combination. For example, maize in the United States is consistently well-simulated while maize in Indonesia is problematic (mean Pearson correlation coefficients of 0.68 and 0.18, respectively). In some cases, especially in the developing world, low
10 correlation coefficients may indicate not only model failure but also problems in FAO yield data (Ray et al., 2012; Müller et al., 2017).

In general, correlation coefficients in GGCMI Phase II are slightly below those of Phase I, likely because of unrealistic nitrogen levels, lack of country level calibration in some models, and restriction to only the MICRA aggregation mask in this study. (Compare Figure 2 to Müller et al. (2017) Figures 1–4 and 6.) Additionally, the time period used in this case is
15 slightly different from the time period used in Müller et al. (2017). Note that in this methodology, simulations of crops with low year-to-year variability such as irrigated rice and wheat will tend to score more poorly than those with higher variability.

3.2 Simulated dynamics and data characteristics

Crop models in the GGCMI Phase II ensemble show broadly consistent responses to climate and management perturbations in most regions, with a strong negative impact of increased temperature in all but the coldest regions. Mapping the distribution
20 of baseline yields and yield changes shows the geographic dependencies that underlie these results. Crop cultivation areas and yield changes with respect to the T+4 scenario show distinct geographic pattern (Figure 3). Absolute yield potentials show strong spatial variation, with much of the Earth’s surface area unsuitable for any of these crops. In general, models agree most on yield response in regions where yield potentials are currently high and therefore where crops are currently grown. Models
25 show robust decreases in yields at low latitudes, and highly uncertain median increases at most high latitudes, due in part to how crop failures are considered across different models. This is also illustrated in Figure 4, which shows that e.g. the PROMET model has a much higher share in crop failure (yield of 0 ton ha⁻¹) at high latitudes (>45° north) than the LPJmL model. For wheat crops see Figure S16. Wheat projections are more uncertain, possibly because simulation calibration is especially important (e.g. Asseng et al., 2013).

Yield response differences at high latitudes are due in part to model representation of zero yields or yield failures. Model
30 representation of crop suitability differs across models for areas where crops not currently grown. For example, soy yields north of 45° in the PROMET model are most often zero in the historical simulations and are relatively evenly distributed between 0

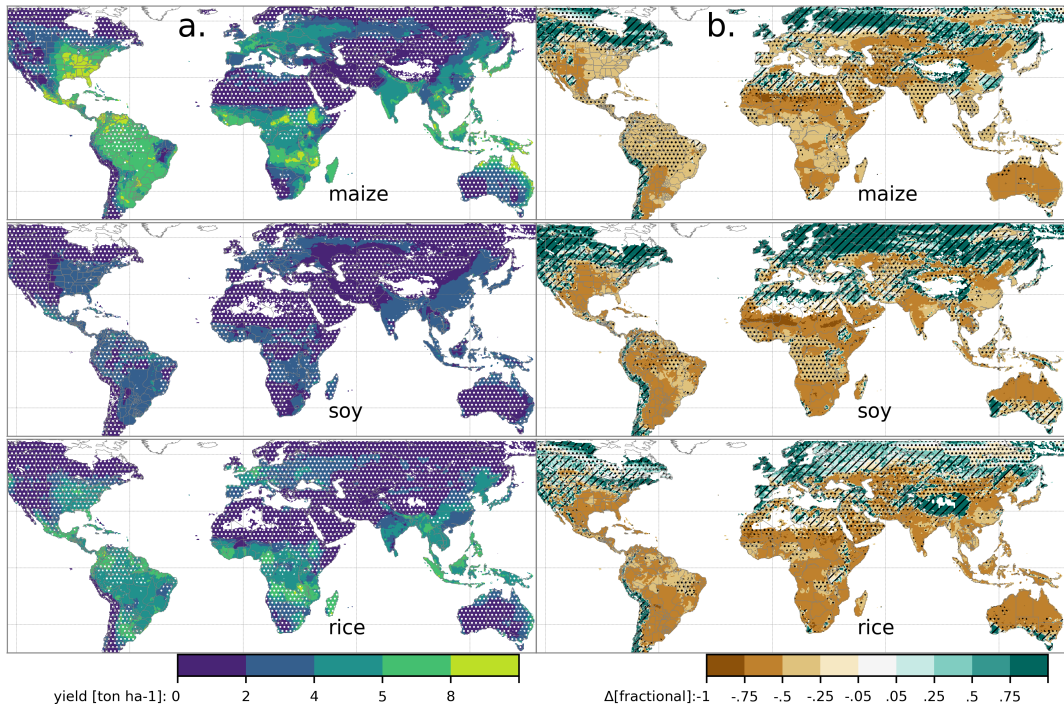


Figure 3. Illustration of the spatial pattern of potential yields and potential yield changes in the GGCMI Phase II ensemble, for three major crops: maize, soybean and rice. Left column (a) shows multi-model mean climatological yields for the baseline scenario for (top–bottom) rainfed maize, soybean, and rice. Wheat shows a qualitatively similar response, see Figure S16 in the supplemental material. White stippling indicates areas where these crops are not currently cultivated. Absence of cultivation aligns well with the lowest yield contour ($0\text{--}2 \text{ ton ha}^{-1}$). Right column (b) shows the multi-model mean fractional yield change in the $T + 4^\circ\text{C}$ scenario (with other inputs at baseline values). Areas without hatching or stippling are those where confidence in projections is high: the multi-model mean fractional change exceeds two standard deviations of the ensemble ($\Delta > 2\sigma$). Hatching indicates areas of low confidence ($\Delta < 1\sigma$), and stippling areas of medium confidence ($1\sigma < \Delta < 2\sigma$). Crop model results in cold areas, where yield impacts are on average positive, also have the highest uncertainty.

and 4 tons ha^{-1} in the LPJmL model. Under the warming scenario ($T+4\text{K}$), many grid cells which were previously too cold to grow soy in the PROMET model are no suitable and the LPJmL yields have shifted slightly down the distribution (Figure 4).

We illustrate the across-model spread for rainfed maize in Figure 5, which shows yields across all grid cells for the primary Köppen-Geiger climate regions (Rubel and Kottek, 2010). In warming scenarios with precipitation held constant, all models show decreases in maize yield in the ‘warm temperate’, ‘equatorial’, and ‘arid’ regions that account for nearly three-quarters 5 of global maize production. These impacts are robust for even moderate climate perturbations. In the ‘warm temperate’ zone, even a 1 degree temperature rise with other variables held fixed leads to a median yield reduction that exceeds the variance across models. A 6 degree temperature rise results in median loss of $\sim 25\%$ of yields with a signal to noise ratio of nearly three to one. A notable exception is the ‘cold continental’ region, where models disagree strongly, extending even to the sign

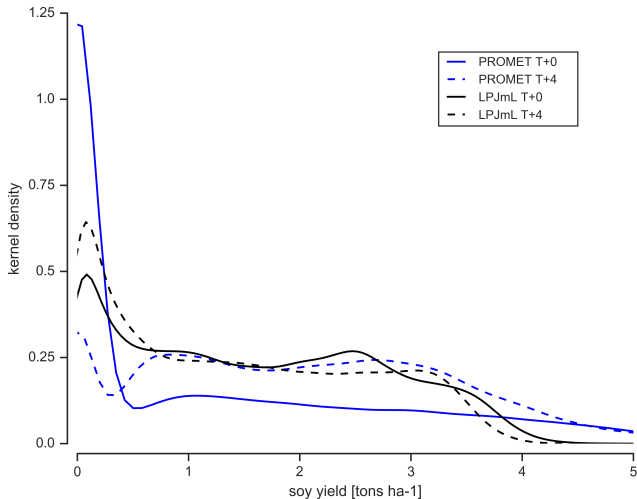


Figure 4. Kernel density estimate of soybean yields north of 45° latitude for the PROMET and LPJmL models. Solid lines show the historical climatology and dashed lines show the T+4 (K) case. Note strong reduction in the lowest bin for the T+4 case for PROMET that is spread almost equally over the rest of the distribution.

of impacts. Other crops show similar responses to warming, with robust yield losses in warmer locations and high inter-model variance in the ‘cold continental’ regions (Figure S5).

The effects of rainfall changes on maize yields shown in Figure 5 (and for soybean in Figure 6) are also relatively consistent across models. Increased rainfall mitigates the negative effect of higher temperatures by counteracting the increased evapo-transpiration to some degree, most strongly in arid regions. Decreased rainfall amplifies yield losses and also increases inter-model variance; i.e. models agree that the response to decreased water availability is negative in sign but disagree on its magnitude. Increased temperature results in a relative flattening of the precipitation change response (Figure 6). We show only rainfed maize and soy here; see Figure S6 for comparison between rainfed and irrigated maize. As expected, irrigated crops are more resilient to temperature increases in all regions, especially so where water is limiting. See Figures S7–15 in the supplement for other crops.

Mean climatological yield response to the other two dimensions (C and N) are qualitatively similar. The yield response to increased CO_2 for spring wheat is a robust increase across models in all climate regions (Figure 7). Increased precipitation allows crops to capture additional yield boost from elevated CO_2 levels in the mid range in most climate regions, but this effect saturates at the highest CO_2 levels. Increased CO_2 outweighs the damages caused by 20% reduced precipitation in all climate regions in the multi-model median, but not all models agree upon the positive sign.

Simulated irrigation water demand, as an example for non-yield outputs, is also variable across models and shows mixed responses to increasing temperatures and generally a decrease with increasing levels of $[\text{CO}_2]$ (Figure 8). This is because shorter growing seasons under warming reduce water demand whereas warmer temperatures increase water demand. Often,

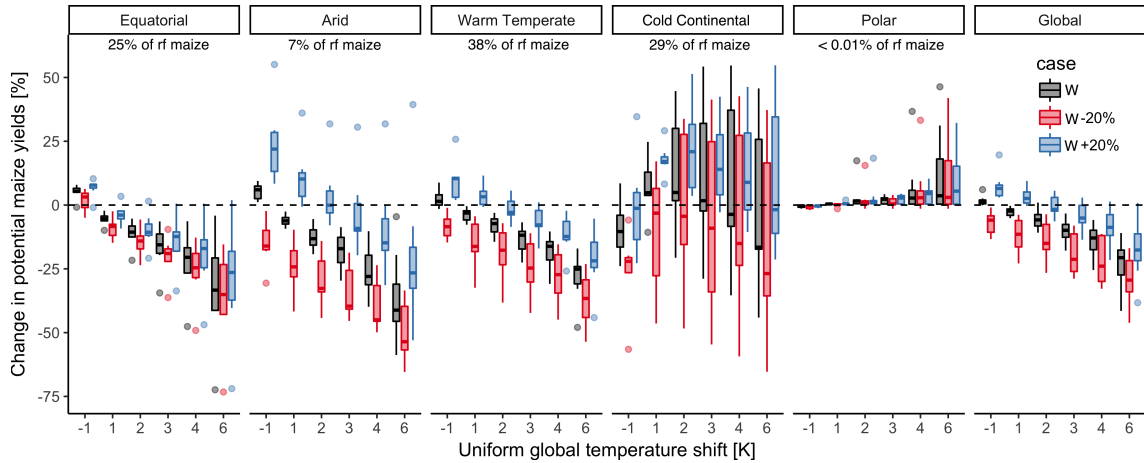


Figure 5. Illustration of the distribution of regional yield changes across the multi-model ensemble, split by Köppen-Geiger climate regions (Rubel and Kottek, 2010). We show responses of a single crop (rainfed maize) to applied uniform temperature perturbations, for three discrete precipitation perturbation levels (-20%, 0%, and +20%), with $[CO_2]$ and nitrogen held constant at baseline values (360 ppm and 200 kg $ha^{-1} yr^{-1}$). Y-axis is fractional change in the regional average climatological potential yield relative to the baseline. Box-and-whiskers plots show distribution across models, with median marked; edges are first and third quartiles, i.e. box height is the interquartile range (IQR). If all models like within 1.5·IQR then whiskers extend to maximum and minimum of simulations, else the outlier is shown separately. Outliers in the tropics (strong negative impact of temperature increases) are the pDSSAT model; outliers in the high-rainfall case (strong positive impact of precipitation increases) are the JULES model. Figure shows all modeled land area; see Figure S4 in the supplemental material for currently-cultivated land and Figure S5 for other crops. Panel text gives the percentage of rainfed maize presently cultivated in each climate zone (data from Portmann et al., 2010). Note that Rubel and Kottek (2010) use the name ‘Snow’ rather than ‘Cold continental’. Outside high-latitude regions (‘Cold continental’ and ‘Polar’), models generally agree, with projected declines under increasing temperatures larger than inter-model variance. The right panel (Global) shows yield responses to a globally uniform temperature shift; note that these results are not directly comparable to simulations of more realistic climate scenarios.

the inter-model uncertainty is larger than the response to warming and can both increase (e.g. Arid) or decrease (e.g. Tropical) with warming.

4 Discussion and Conclusions

The GGCMII Phase II experiment provides a database designed to allow detailed study of crop yields from process-based models under climate change. The use of systematic input parameter variations facilitates not only comparing the sensitivities of process-based crop yield models to changing climate and management inputs but also evaluating the complex interactions between driving factors ($[CO_2]$, temperature, precipitation, and applied nitrogen). Its global extent also allows identifying geographic shifts in high yield potential locations. We expect that the simulations will yield multiple insights in future studies, and show a selection of preliminary results. We discuss below the implications from the experimental design, but refrain from

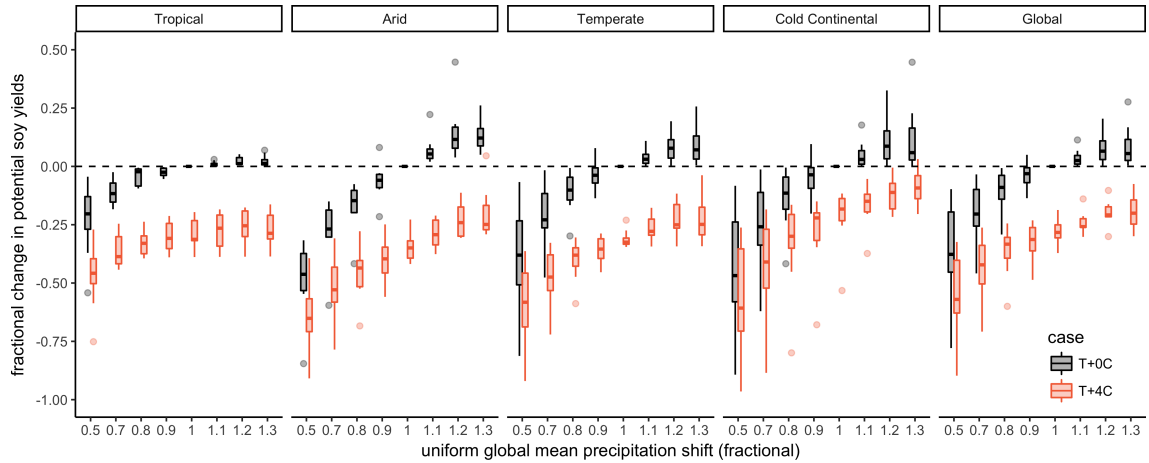


Figure 6. Illustration of the distribution of regional yield changes across the multi-model ensemble, split by Köppen-Geiger climate regions for soybean. Same conventions as Figure 5 except precipitation is varied. Simulations at a T + 4K are show in color.

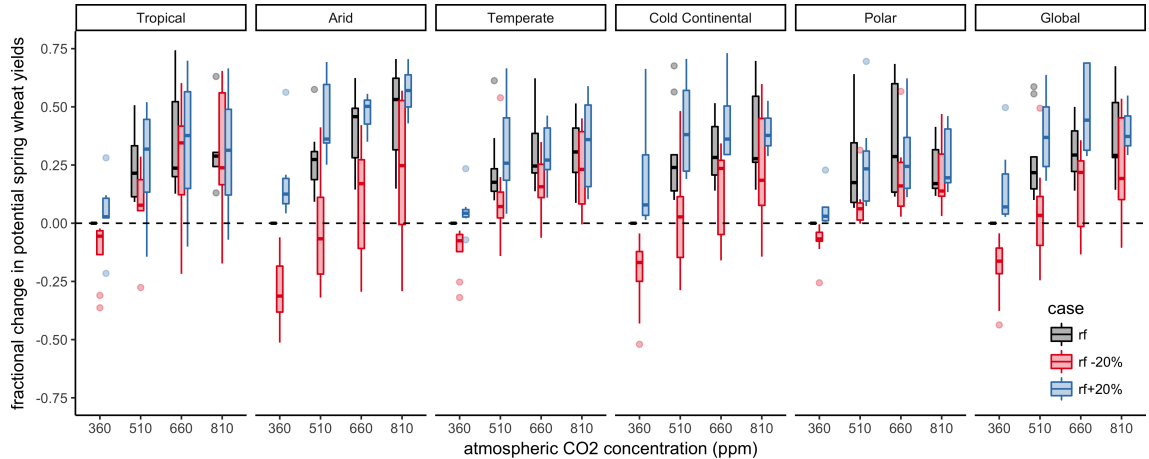


Figure 7. Illustration of the distribution of regional yield changes across the multi-model ensemble, split by Köppen-Geiger climate regions for spring wheat. Same conventions as Figure 5 except atmospheric carbon dioxide is varied. Two different water specifications (historical precipitation -20% and +20%) are shown in colors.

analyzing simulation results in detail. Data analyses will be conducted in subsequent analyses making use of the GGCMI Phase II data archive.

First, the GGCMI Phase II simulations allow identifying major areas of uncertainty. Inter-model uncertainty is qualitatively similar across all four inputs tested at the globally aggregate level with some notable exceptions. For example, soybean, a nitrogen-fixing legume, is insensitive to nitrogen addition, while wheat is particularly uncertain in its response to [CO₂] levels and water availability (Figure S22). Across geographic regions, projections are most robust in the low latitudes where yield

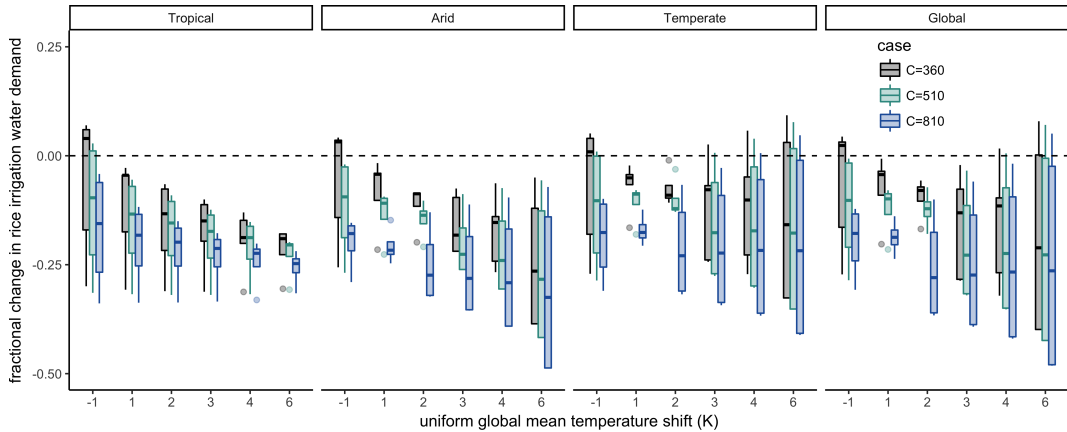


Figure 8. Illustration of the distribution of regional irrigation water demand across the multi-model ensemble, split by Köppen-Geiger climate regions for rice. Cold continental and polar regions are not shown because very little rice is grown in these regions.

impacts are largest, and most uncertain in the high latitudes where yields may increase under warming. Model differences in projected high-latitude yield changes appear driven more by differences in baseline than in responses to CTWN perturbations. PROMET, for example, involves a stronger response to cold than does LPJmL, with frost below -8°C irreversibly killing non-winter crops and prolonged periods of below-optimum temperatures also leading to complete crop failure. Over the high-latitudes regions simulated by both models, 52% of grid cells in PROMET report 0 yield in the present climate vs. 11% of cells in the T+4 scenario, leading to a strong yield gain in warmer future climates. In LPJmL outputs, the same high-latitude area is deemed suitable for cultivation even in baseline climate, with crop failure rates of 4% and 5% in present and T+4 cases, so that projected yield changes are modest (Figure 4.).

Second, the GGCMI Phase II simulations demonstrate the sensitivity of climate-driven yield impacts to the locations of cultivated land. One counterintuitive result apparent in the simulations is that warmer temperatures drive steeper yield reductions in irrigated than rainfed maize when considered only over currently cultivated land, even though water availability increases crop resiliency to temperature increases at any given location (compare Figure 5 and Figures S6 to S7). The effect results from geographic differences in cultivation: irrigated maize is grown in warmer locations where the impacts of warming are more severe (See Figures S8-S15 for other crops.) Geographic effects also mean that nitrogen fertilization produces stronger responses in irrigated than non-irrigated wheat and maize, presumably because those rainfed crops are limited by water availability (Figure S21).

In general, the development of multi-model ensembles involving systematic parameters sweeps has large promise for increasing understanding of potential future crop responses and for improving process-based crop models. The data set is unprecedentedly large, being global in extent, covering 31-simulation years per pixel and up to 756 perturbations for 12 GGCMS. We expect that the GGCMI Phase II data archive will be used to analyze the different GGCMS' sensitivity to changes in the

CTWN-A space, including the interaction between drivers. The authors are working on some analyses but many more are

20 facilitated by the GGCMI Phase II data archive.

Code and data availability. The simulation outputs of the mandatory 7 output variables (Table 2) are available on zenodo.org. See Appendix A1 for data DOIs. All other simulation output variables are available upon request to the corresponding author. The scripts for generating the spring wheat and winter wheat growing seasons and second fertilizer dates and the quality screening script is available at <https://github.com/RDCEP/ggcmi/blob/phase2/>. All input data are available via globus.org (registration required, free of charge): Minimum cropland mask is available at https://www.globus.org/app/transfer?origin_id=e4c16e81-6d04-11e5-ba46-22000b92c6ec&origin_path=%2FAGMIP.input%2FCTWN%2F choose the file boolean_cropmask_ggcmi_phase2.nc4 Growing period data for wheat is now divided up into winter and spring wheat, available at https://www.globus.org/app/transfer?origin_id=e4c16e81-6d04-11e5-ba46-22000b92c6ec&origin_path=%2FAGMIP.input%2Fother.inputs%2FAGMIP_GROWING_SEASON.HARM.version2.0%2F whereas all other growing season data (maize, rice, soybean) are the same as in Phase I (version 1.25), available at https://www.globus.org/app/transfer?origin_id=e4c16e81-6d04-11e5-ba46-22000b92c6ec&origin_path=%2FAGMIP.input%2Fother.inputs%2FAGMIP_GROWING_SEASON.HARM.version1.25%2F

Appendix A

A1 Data Access

Simulation yield output datasets can be found at the DOIs located in table A1. Data are published in crop- and GGCM-specific packages, in order to break down the overall data amount into manageable packages (<50GB per archive).

Author contributions. J.E., C.M, and A.R. designed the research. C.M., J.J., J.B., P.C., M.D., P.F., C.F., L.F., M.H., C.I., I.J., C.J., N.K., M.K., W.L., S.O., M.P., T.P., A.R., X.W., K.W., and F.Z. performed the simulations. J.F., J.J., A.S., M.L., C.M., and E.M. performed the analysis and J.F., E.M., and C.M. prepared the manuscript.

Competing interests. The authors declare no competing interests.

20 *Acknowledgements.* This research was performed as part of the Center for Robust Decision-Making on Climate and Energy Policy (RDCEP) at the University of Chicago, and was supported through a variety of sources. RDCEP is funded by NSF grant #SES-1463644 through the Decision Making Under Uncertainty program. J.F. was supported by the NSF NRT program, grant #DGE-1735359. C.M. was supported by the MACMIT project (01LN1317A) funded through the German Federal Ministry of Education and Research (BMBF). C.F. was supported by the European Research Council Synergy grant #ERC-2013-SyG-610028 Imbalance-P. P.F. and K.W. were supported by the Newton Fund

Table A1. DOI's for model yield data outputs. All yield output data can be found at <https://doi.org/10.5281/zenodo/XX>. Where XX is the value found in the table.

Model	Maize	Soybean	Rice	Winter wheat	Spring wheat
APSIM-UGOE	2582531	2582535	2582533	2582537	2582539
CARAIB	2582522	2582508	2582504	2582516	2582499
EPIC-IIASA	2582453	2582461	2582457	2582463	2582465
EPIC-TAMU	2582349	2582367	2582352	2582392	2582418
JULES	2582543	2582547	2582545	–	2582551
GEPIC	2582247	2582258	2582251	2582260	2582263
LPJ-GUESS	2581625	–	–	2581638	2581640
LPJmL	2581356	2581498	2581436	2581565	2581606
ORCHIDEE-crop	2582441	–	2582445	2582449	–
pDSSAT	2582111	2582147	2582127	2582163	2582178
PEPIC	2582341	2582433	2582343	2582439	2582455
PROMET	2582467	2582488	2582479	2582490	2582492

- 25 through the Met Office Climate Science for Service Partnership Brazil (CSSP Brazil). K.W. was supported by the IMPREX research project supported by the European Commission under the Horizon 2020 Framework programme, grant #641811. A.S. was supported by the Office of Science of the U.S. Department of Energy as part of the Multi-sector Dynamics Research Program Area. S.O. acknowledges support from the Swedish strong research areas BECC and MERGE together with support from LUCCI (Lund University Centre for studies of Carbon Cycle and Climate Interactions). R.C.I. acknowledges support from the Texas Agrilife Research and 634 Extension, Texas A & M University.
- 5 This is paper number 35 of the Birmingham Institute of Forest Research. Computing resources were provided by the University of Chicago Research Computing Center (RCC).

References

- Angulo, C., Rötter, R., Lock, R., Enders, A., Fronzek, S., and Ewert, F.: Implication of crop model calibration strategies for assessing regional impacts of climate change in Europe, *Agric. For. Meteorol.*, 170, 32 – 46, <https://doi.org/10.1016/j.agrformet.2012.11.017>, 2013.
- 10 Asseng, S., Ewert, F., Rosenzweig, C., Jones, J., Hatfield, J., Ruane, A., J. Boote, K., Thorburn, P., Rötter, R. P., Cammarano, D., Brisson, N., Basso, B., Martre, P., Aggarwal, P., Angulo, C., Bertuzzi, P., Biernath, C., Challinor, A., Doltra, J., Gayler, S., Goldberg, R., Grant, R., Heng, L., Hooker, J., Hunt, L. A., Ingwersen, J., Izaurralde, R. C., Kersebaum, K. C., Müller, C., Kumar, S. N., Nendel, C., Leary, G. O., Olesen, J. E., Osborne, T. M., Palosuo, T., Priesack, E., Riponche, D., Semenov, M. A., Shcherbak, I., Steduto, P., Stöckle, C., Strattonovitch, P., Streck, T., Supit, I., Tao, F., Travasso, M., Waha, K., Wallach, D., Williams, J. R., and Wolf, J.: Uncertainty in simulating wheat yields under climate change, *Nature Climate Change*, 3, 827–832, <https://doi.org/10.1038/nclimate1916>, 2013.
- Asseng, S., Ewert, F., Martre, P., Rötter, R. P., B. Lobell, D., Cammarano, D., A. Kimball, B., Ottman, M., W. Wall, G., White, J., Reynolds, 5 M., D. Alderman, P., Prasad, P. V. V., Aggarwal, P., Anothai, J., Basso, B., Biernath, C., Challinor, A., De Sanctis, G., Doltra, J., Fereres, E., Garcia-Vila, M., Gayler, S., Hoogenboom, G., Hunt, L. A., Izaurralde, R. C., Jabloun, M., Jones, C. D., Kersebaum, K. C., Koehler, A.-K., Muller, C., Naresh Kumar, S., Nendel, C., O'Leary, G., Olesen, J. E., Palosuo, T., Priesack, E., Eyshi Rezaei, E., Ruane, A. C., Semenov, M. A., Shcherbak, I., Stockle, C., Strattonovitch, P., Streck, T., Supit, I., Tao, F., Thorburn, P. J., Waha, K., Wang, E., Wallach, D., Wolf, J., Zhao, Z., and Zhu, Y.: Rising temperatures reduce global wheat production, *Nature Climate Change*, 5, 143–147, 10 <https://doi.org/10.1038/nclimate2470>, 2015.
- Balkovič, J., van der Velde, M., Skalský, R., Xiong, W., Folberth, C., Khabarov, N., Smirnov, A., Mueller, N. D., and Obersteiner, M.: Global wheat production potentials and management flexibility under the representative concentration pathways, *Global and Planetary Change*, 122, 107 – 121, <https://doi.org/10.1016/j.gloplacha.2014.08.010>, 2014.
- Bodirsky, B. L., Rolinski, S., Biewald, A., Weindl, I., Popp, A., and Lotze-Campen, H.: Global Food Demand Scenarios for the 21st Century, 15 PLOS ONE, 10, 1–27, <https://doi.org/10.1371/journal.pone.0139201>, <https://doi.org/10.1371/journal.pone.0139201>, 2015.
- Challinor, A., Watson, J., Lobell, D., Howden, S., Smith, D., and Chhetri, N.: A meta-analysis of crop yield under climate change and adaptation, *Nature Climate Change*, 4, 287 – 291, <https://doi.org/10.1038/nclimate2153>, 2014.
- Challinor, A. J., Müller, C., Asseng, S., Deva, C., Nicklin, K. J., Wallach, D., Vanuytrecht, E., Whitfield, S., Ramirez-Villegas, J., and Koehler, A.-K.: Improving the use of crop models for risk assessment and climate change adaptation, *Agricultural systems*, 159, 296–306, 2018.
- 20 Dee, D. P., Uppala, S., Simmons, A., Berrisford, P., Poli, P., Kobayashi, S., Andrae, U., Balmaseda, M., Balsamo, G., Bauer, d. P., et al.: The ERA-Interim reanalysis: Configuration and performance of the data assimilation system, *Quarterly Journal of the royal meteorological society*, 137, 553–597, 2011.
- Dury, M., Hambuckers, A., Warnant, P., Henrot, A., Favre, E., Ouberdoos, M., and François, L.: Responses of European forest ecosystems to 21st century climate: assessing changes in interannual variability and fire intensity, *iForest - Biogeosciences and Forestry*, pp. 82–99, 25 <https://doi.org/10.3832/ifor0572-004>, 2011.
- Elliott, J., Kelly, D., Chryssanthacopoulos, J., Glotter, M., Jhunjhnuwala, K., Best, N., Wilde, M., and Foster, I.: The parallel system for integrating impact models and sectors (pSIMS), *Environmental Modelling and Software*, 62, 509–516, <https://doi.org/10.1016/j.envsoft.2014.04.008>, 2014.
- Elliott, J., Müller, C., Deryng, D., Chryssanthacopoulos, J., Boote, K. J., Büchner, M., Foster, I., Glotter, M., Heinke, J., Iizumi, T., Izaurralde, R. C., Mueller, N. D., Ray, D. K., Rosenzweig, C., Ruane, A. C., and Sheffield, J.: The Global Gridded Crop Model Intercomparison: data and modeling protocols for Phase 1 (v1.0), *Geoscientific Model Development*, 8, 261–277, <https://doi.org/10.5194/gmd-2016-207>, 2015.

Eyring, V., Bony, S., Meehl, G. A., Senior, C. A., Stevens, B., Stouffer, R. J., and Taylor, K. E.: Overview of the Coupled Model Intercomparison Project Phase 6 (CMIP6) experimental design and organization, *Geoscientific Model Development*, 9, 1937–1958, <https://doi.org/10.5194/gmdd-8-10539-2015>, 2016.

35 Folberth, C., Gaiser, T., Abbaspour, K. C., Schulin, R., and Yang, H.: Regionalization of a large-scale crop growth model for sub-Saharan Africa: Model setup, evaluation, and estimation of maize yields, *Agriculture, Ecosystems & Environment*, 151, 21 – 33, <https://doi.org/10.1016/j.agee.2012.01.026>, 2012.

Folberth, C., Elliott, J., Müller, C., Balkovic, J., Chryssanthacopoulos, J., Izaurrealde, R. C., Jones, C. D., Khabarov, N., Liu, W., Reddy, A., Schmid, E., Skalský, R., Yang, H., Arneth, A., Ciais, P., Deryng, D., Lawrence, P. J., Olin, S., Pugh, T. A. M., Ruane, A. C., and Wang, X.: Uncertainties in global crop model frameworks: effects of cultivar distribution, crop management and soil handling on crop yield estimates, *Biogeosciences Discussions*, 2016, 1–30, <https://doi.org/10.5194/bg-2016-527>, <https://www.biogeosciences-discuss.net/bg-2016-527/>, 2016.

5 Food and Agriculture Organization of the United Nations: FAOSTAT Database, <http://www.fao.org/faostat/en/home>, 2018.

Frieler, K., Lange, S., Piontek, F., Reyer, C. P., Schewe, J., Warszawski, L., Zhao, F., Chini, L., Denvil, S., Emanuel, K., et al.: Assessing the impacts of 1.5 C global warming—simulation protocol of the Inter-Sectoral Impact Model Intercomparison Project (ISIMIP2b), *Geoscientific Model Development*, 2017.

10 Glotter, M., Elliott, J., McInerney, D., Best, N., Foster, I., and Moyer, E. J.: Evaluating the utility of dynamical downscaling in agricultural impacts projections, *Proceedings of the National Academy of Sciences*, 111, 8776–8781, <https://doi.org/10.1073/pnas.1314787111>, 2014.

Glotter, M., Moyer, E., Ruane, A., and Elliott, J.: Evaluating the Sensitivity of Agricultural Model Performance to Different Climate Inputs, *Journal of Applied Meteorology and Climatology*, 55, 151113145618001, <https://doi.org/10.1175/JAMC-D-15-0120.1>, 2015.

Hank, T., Bach, H., and Mauser, W.: Using a Remote Sensing-Supported Hydro-Agroecological Model for Field-Scale Simulation of Heterogeneous Crop Growth and Yield: Application for Wheat in Central Europe, *Remote Sensing*, 7, 3934–3965, <https://doi.org/10.3390/rs70403934>, 2015.

15 Hasegawa, T., Fujimori, S., Havlík, P., Valin, H., Bodirsky, B. L., Doelman, J. C., Fellmann, T., Kyle, P., Koopman, J. F., Lotze-Campen, H., et al.: Risk of increased food insecurity under stringent global climate change mitigation policy, *Nature Climate Change*, 8, 699, 2018.

Holzworth, D. P., Huth, N. I., deVoil, P. G., Zurcher, E. J., Herrmann, N. I., McLean, G., Chenu, K., van Oosterom, E. J., Snow, V., Murphy, C., Moore, A. D., Brown, H., Whish, J. P., Verrall, S., Fainges, J., Bell, L. W., Peake, A. S., Poulton, P. L., Hochman, Z., Thorburn, P. J., Gaydon, D. S., Dalgliesh, N. P., Rodriguez, D., Cox, H., Chapman, S., Doherty, A., Teixeira, E., Sharp, J., Cichota, R., Vogeler, I., Li, F. Y., Wang, E., Hammer, G. L., Robertson, M. J., Dimes, J. P., Whitbread, A. M., Hunt, J., van Rees, H., McClelland, T., Carberry, P. S., Hargreaves, J. N., MacLeod, N., McDonald, C., Harsdorf, J., Wedgwood, S., and Keating, B. A.: APSIM – Evolution towards a new generation of agricultural systems simulation, *Environmental Modelling and Software*, 62, 327 – 350, <https://doi.org/10.1016/j.envsoft.2014.07.009>, 2014.

20 Humpenöder, F., Popp, A., Bodirsky, B. L., Weindl, I., Biewald, A., Lotze-Campen, H., Dietrich, J. P., Klein, D., Kreidenweis, U., Müller, C., et al.: Large-scale bioenergy production: how to resolve sustainability trade-offs?, *Environmental Research Letters*, 13, 024011, 2018.

Iizumi, T., Nishimori, M., and Yokozawa, M.: Diagnostics of Climate Model Biases in Summer Temperature and Warm-Season Insolation for the Simulation of Regional Paddy Rice Yield in Japan, *Journal of Applied Meteorology and Climatology*, 49, 574–591, <https://doi.org/10.1175/2009JAMC2225.1>, 2010.

- Iizumi, T., Yokozawa, M., Sakurai, G., Travasso, M. I., Romanenkov, V., Oettli, P., Newby, T., Ishigooka, Y., and Furuya, J.: Historical changes in global yields: major cereal and legume crops from 1982 to 2006, *Global Ecology and Biogeography*, 23, 346–357, <https://doi.org/10.1111/geb.12120>, 2014.
- Izaurrealde, R., Williams, J., McGill, W., Rosenberg, N., and Quiroga Jakas, M.: Simulating soil C dynamics with EPIC: Model description and testing against long-term data, *Ecological Modelling*, 192, 362–384, <https://doi.org/10.1016/j.ecolmodel.2005.07.010>, 2006.
- J. Boote, K., Jones, J., White, J., Asseng, S., and Lizaso, J.: Putting Mechanisms into Crop Production Models., *Plant, cell & environment*, 36, <https://doi.org/10.1111/pce.12119>, 2013.
- Jägermeyr, J. and Frieler, K.: Spatial variations in crop growing seasons pivotal to reproduce global fluctuations in maize and wheat yields, *Science Advances*, 4, 4517, <https://doi.org/10.1126/sciadv.aat4517>, 2018.
- Jagtap, S. S. and Jones, J. W.: Adaptation and evaluation of the CROPGRO-soybean model to predict regional yield and production, *Agriculture, Ecosystems & Environment*, 93, 73 – 85, [https://doi.org/10.1016/S0167-8809\(01\)00358-9](https://doi.org/10.1016/S0167-8809(01)00358-9), 2002.
- Jones, J., Hoogenboom, G., Porter, C., Boote, K., Batchelor, W., Hunt, L., Wilkens, P., Singh, U., Gijsman, A., and Ritchie, J.: The DSSAT cropping system model, *European Journal of Agronomy*, 18, 235 – 265, [https://doi.org/10.1016/S1161-0301\(02\)00107-7](https://doi.org/10.1016/S1161-0301(02)00107-7), 2003.
- Jones, J. W., Antle, J. M., Basso, B., Boote, K. J., Conant, R. T., Foster, I., Godfray, H. C. J., Herrero, M., Howitt, R. E., Janssen, S., Keating, B. A., Munoz-Carpena, R., Porter, C. H., Rosenzweig, C., and Wheeler, T. R.: Toward a new generation of agricultural system data, models, and knowledge products: State of agricultural systems science, *Agricultural Systems*, 155, 269 – 288, <https://doi.org/doi.org/10.1016/j.agrsy.2016.09.021>, 2017.
- Keating, B., Carberry, P., Hammer, G., Probert, M., Robertson, M., Holzworth, D., Huth, N., Hargreaves, J., Meinke, H., Hochman, Z., McLean, G., Verburg, K., Snow, V., Dimes, J., Silburn, M., Wang, E., Brown, S., Bristow, K., Asseng, S., Chapman, S., McCown, R., Freebairn, D., and Smith, C.: An overview of APSIM, a model designed for farming systems simulation, *European Journal of Agronomy*, 18, 267 – 288, [https://doi.org/10.1016/S1161-0301\(02\)00108-9](https://doi.org/10.1016/S1161-0301(02)00108-9), 2003.
- Lindeskog, M., Arneth, A., Bondeau, A., Waha, K., Seaquist, J., Olin, S., and Smith, B.: Implications of accounting for land use in simulations of ecosystem carbon cycling in Africa, *Earth System Dynamics*, 4, 385–407, <https://doi.org/10.5194/esd-4-385-2013>, 2013.
- Liu, J., Williams, J. R., Zehnder, A. J., and Yang, H.: GEPIC - modelling wheat yield and crop water productivity with high resolution on a global scale, *Agricultural Systems*, 94, 478 – 493, <https://doi.org/10.1016/j.agrsy.2006.11.019>, 2007.
- Liu, W., Yang, H., Folberth, C., Wang, X., Luo, Q., and Schulin, R.: Global investigation of impacts of PET methods on simulating crop-water relations for maize, *Agricultural and Forest Meteorology*, 221, 164 – 175, <https://doi.org/10.1016/j.agrformet.2016.02.017>, 2016a.
- Liu, W., Yang, H., Liu, J., Azevedo, L. B., Wang, X., Xu, Z., Abbaspour, K. C., and Schulin, R.: Global assessment of nitrogen losses and trade-offs with yields from major crop cultivations, *Science of The Total Environment*, 572, 526 – 537, <https://doi.org/10.1016/j.scitotenv.2016.08.093>, 2016b.
- Mauser, W., Klepper, G., Zabel, F., Delzeit, R., Hank, T., Putzenlechner, B., and Calzadilla, A.: Global biomass production potentials exceed expected future demand without the need for cropland expansion, *Nature Communications*, 6, <https://doi.org/10.1038/ncomms9946>, 2015.
- McDermid, S. P., Ruane, A. C., Rosenzweig, C., Hudson, N. I., Morales, M. D., Agalawatte, P., Ahmad, S., Ahuja, L., Amien, I., Anapalli, S. S., et al.: The AgMIP coordinated climate-crop modeling project (C3MP): methods and protocols, in: *HANDBOOK OF CLIMATE CHANGE AND AGROECOSYSTEMS: The Agricultural Model Intercomparison and Improvement Project Integrated Crop and Economic Assessments*, Part 1, pp. 191–220, World Scientific, 2015.
- Minoli, S., Egli, D. B., Rolinski, S., and Müller, C.: Modelling cropping periods of grain crops at the global scale, *Global and Planetary Change*, 174, 35–46, 2019.

Müller, C., Elliott, J., Chryssanthacopoulos, J., Deryng, D., Folberth, C., Pugh, T. A., and Schmid, E.: Implications of climate mitigation for future agricultural production, *Environmental Research Letters*, 10, 125 004, 2015.

35 Müller, C., Elliott, J., Chryssanthacopoulos, J., Arneth, A., Balkovic, J., Ciais, P., Deryng, D., Folberth, C., Glotter, M., Hoek, S., Iizumi, T., Izaurrealde, R. C., Jones, C., Khabarov, N., Lawrence, P., Liu, W., Olin, S., Pugh, T. A. M., Ray, D. K., Reddy, A., Rosenzweig, C., Ruane, A. C., Sakurai, G., Schmid, E., Skalsky, R., Song, C. X., Wang, X., de Wit, A., and Yang, H.: Global gridded crop model evaluation: benchmarking, skills, deficiencies and implications, *Geoscientific Model Development*, 10, 1403–1422, <https://doi.org/10.5194/gmd-10-1403-2017>, 2017.

Olesen, J. E., Børgesen, C. D., Elsgaard, L., Palosuo, T., Rötter, R., Skjelvåg, A., Peltonen-Sainio, P., Börjesson, T., Trnka, M., Ewert, F., et al.: Changes in time of sowing, flowering and maturity of cereals in Europe under climate change, *Food Additives & Contaminants: Part A*, 29, 1527–1542, 2012.

5 Olin, S., Schurges, G., Lindeskog, M., Wårild, D., Smith, B., Bodin, P., Holmér, J., and Arneth, A.: Modelling the response of yields and tissue C:N to changes in atmospheric CO₂ and N management in the main wheat regions of western Europe, *Biogeosciences*, 12, 2489–2515, <https://doi.org/10.5194/bg-12-2489-2015>, 2015.

Osborne, T., Gornall, J., Hooker, J., Williams, K., Wiltshire, A., Betts, R., and Wheeler, T.: JULES-crop: a parametrisation of crops in the Joint UK Land Environment Simulator, *Geoscientific Model Development*, 8, 1139–1155, <https://doi.org/10.5194/gmd-8-1139-2015>, 10 2015.

Pirttioja, N., Carter, T., Fronzek, S., Bindi, M., Hoffmann, H., Palosuo, T., Ruiz-Ramos, M., Tao, F., Trnka, M., Acutis, M., Asseng, S., Baranowski, P., Basso, B., Bodin, P., Buis, S., Cammarano, D., Deligios, P., Destain, M., Dumont, B., Ewert, F., Ferrise, R., François, L., Gaiser, T., Hlavinka, P., Jacquemin, I., Kersebaum, K., Kollas, C., Krzyszczak, J., Lorite, I., Minet, J., Minguez, M., Montesino, M., Moriondo, M., Müller, C., Nendel, C., Öztürk, I., Perego, A., Rodríguez, A., Ruane, A., Ruget, F., Sanna, M., Semenov, M., Slawinski, C., Stratonovitch, P., Supit, I., Waha, K., Wang, E., Wu, L., Zhao, Z., and Rötter, R.: Temperature and precipitation effects on wheat yield across a European transect: a crop model ensemble analysis using impact response surfaces, *Climate Research*, 65, 87–105, <https://doi.org/10.3354/cr01322>, 2015.

Porter et al. (IPCC): Food security and food production systems. *Climate Change 2014: Impacts, Adaptation, and Vulnerability. Part A: Global and Sectoral Aspects. Contribution of Working Group II to the Fifth Assessment Report of the Intergovernmental Panel on Climate Change*, in: IPCC Fifth Assessment Report, edited by et al., C. F. pp. 485–533, Cambridge University Press, Cambridge, UK, 2014.

Portmann, F., Siebert, S., Bauer, C., and Doell, P.: Global dataset of monthly growing areas of 26 irrigated crops, <https://doi.org/>, 2008.

Portmann, F., Siebert, S., and Doell, P.: MIRCA2000 - Global Monthly Irrigated and Rainfed Crop Areas around the Year 2000: A New High-Resolution Data Set for Agricultural and Hydrological Modeling, *Global Biogeochemical Cycles*, 24, GB1011, <https://doi.org/10.1029/2008GB003435>, 2010.

25 Porwollik, V., Müller, C., Elliott, J., Chryssanthacopoulos, J., Iizumi, T., Ray, D. K., Ruane, A. C., Arneth, A., Balkovič, J., Ciais, P., Deryng, D., Folberth, C., Izaurrealde, R. C., Jones, C. D., Khabarov, N., Lawrence, P. J., Liu, W., Pugh, T. A., Reddy, A., Sakurai, G., Schmid, E., Wang, X., de Wit, A., and Wu, X.: Spatial and temporal uncertainty of crop yield aggregations, *European Journal of Agronomy*, 88, 10–21, <https://doi.org/10.1016/j.eja.2016.08.006>, 2017.

30 Pugh, T., Müller, C., Elliott, J., Deryng, D., Folberth, C., Olin, S., Schmid, E., and Arneth, A.: Climate analogues suggest limited potential for intensification of production on current croplands under climate change, *Nature Communications*, 7, 12608, <https://doi.org/10.1038/ncomms12608>, 2016.

- Ray, D., Ramankutty, N., Mueller, N., West, P., and A Foley, J.: Recent patterns of crop yield growth and stagnation, *Nature communications*, 3, 1293, <https://doi.org/10.1038/ncomms2296>, 2012.
- Roberts, M., Braun, N., R Sinclair, T., B Lobell, D., and Schlenker, W.: Comparing and combining process-based crop models and statistical
35 models with some implications for climate change, *Environmental Research Letters*, 12, <https://doi.org/10.1088/1748-9326/aa7f33>, 2017.
- Rosenzweig, C., Jones, J., Hatfield, J., Ruane, A., Boote, K., Thorburn, P., Antle, J., Nelson, G., Porter, C., Janssen, S., Asseng, S., Basso, B., Ewert, F., Wallach, D., Baigorria, G., and Winter, J.: The Agricultural Model Intercomparison and Improvement Project (AgMIP): Protocols and pilot studies, *Agricultural and Forest Meteorology*, 170, 166 – 182, <https://doi.org/10.1016/j.agrformet.2012.09.011>, 2013.
- Rosenzweig, C., Elliott, J., Deryng, D., Ruane, A. C., Müller, C., Arneth, A., Boote, K. J., Folberth, C., Glotter, M., Khabarov, N., Neumann, K., Piontek, F., Pugh, T. A. M., Schmid, E., Stehfest, E., Yang, H., and Jones, J. W.: Assessing agricultural risks of climate change in the 21st century in a global gridded crop model intercomparison, *Proceedings of the National Academy of Sciences*, 111, 3268–3273,
5 <https://doi.org/10.1073/pnas.1222463110>, 2014.
- Rosenzweig, C., Ruane, A. C., Antle, J., Elliott, J., Ashfaq, M., Chatta, A. A., Ewert, F., Folberth, C., Hathie, I., Havlik, P., Hoogenboom, G., Lotze-Campen, H., MacCarthy, D. S., Mason-D'Croz, D., Contreras, E. M., Müller, C., Perez-Dominguez, I., Phillips, M., Porter, C., Raymundo, R. M., Sands, R. D., Schleussner, C.-F., Valdivia, R. O., Valin, H., and Wiebe, K.: Coordinating AgMIP data and models across global and regional scales for 1.5°C and 2.0°C assessments, *Philosophical Transactions of the Royal Society of London A: Mathematical, Physical and Engineering Sciences*, 376, <https://doi.org/10.1098/rsta.2016.0455>, 2018.
- Rötter, R. P., Carter, T. R., Olesen, J. E., and Porter, J. R.: Crop-climate models need an overhaul, *Nature climate change*, 1, 175, 2011.
- Ruane, A. C., McDermid, S., Rosenzweig, C., Baigorria, G. A., Jones, J. W., Romero, C. C., and Cecil, L. D.: Carbon-temperature-water
change analysis for peanut production under climate change: A prototype for the AgMIP Coordinated Climate-Crop Modeling Project (C3MP), *Glob. Change Biology*, 20, 394–407, <https://doi.org/10.1111/gcb.12412>, 2014.
- Ruane, A. C., Goldberg, R., and Chryssanthacopoulos, J.: Climate forcing datasets for agricultural modeling: Merged products for gap-filling
15 and historical climate series estimation, *Agric. Forest Meteorol.*, 200, 233–248, <https://doi.org/10.1016/j.agrformet.2014.09.016>, 2015.
- Ruane, A. C., Antle, J., Elliott, J., Folberth, C., Hoogenboom, G., Mason-D'Croz, D., Müller, C., Porter, C., Phillips, M. M., Raymundo,
R. M., Sands, R., Valdivia, R. O., White, J. W., Wiebe, K., and Rosenzweig, C.: Biophysical and economic implications for agriculture of +1.5° and +2.0°C global warming using AgMIP Coordinated Global and Regional Assessments, *Climate Research*, 76, 17–39,
20 <https://doi.org/10.3354/crf01520>, 2018.
- Rubel, F. and Kottek, M.: Observed and projected climate shifts 1901–2100 depicted by world maps of the Köppen-Geiger climate classification, *Meteorologische Zeitschrift*, 19, 135–141, <https://doi.org/10.1127/0941-2948/2010/0430>, 2010.
- Sacks, W. J., Deryng, D., Foley, J. A., and Ramankutty, N.: Crop planting dates: an analysis of global patterns, *Global Ecology and Biogeography*, 19, 607–620, <https://doi.org/10.1029/2009GB003765>, 2010.
- Schauberger, B., Archontoulis, S., Arneth, A., Balkovic, J., Ciais, P., Deryng, D., Elliott, J., Folberth, C., Khabarov, N., Müller, C.,
A. M. Pugh, T., Rolinski, S., Schaphoff, S., Schmid, E., Wang, X., Schlenker, W., and Frieler, K.: Consistent negative response of US
25 crops to high temperatures in observations and crop models, *Nature Communications*, 8, 13 931, <https://doi.org/10.1038/ncomms13931>, 2017.
- Schewe, J., Gosling, S. N., Reyer, C., Zhao, F., Ciais, P., Elliott, J., Francois, L., Huber, V., Lotze, H. K., Seneviratne, S. I., van Vliet, M.
T. H., Vautard, R., Wada, Y., Breuer, L., Büchner, M., Carozza, D. A., Chang, J., Coll, M., Deryng, D., de Wit, A., Eddy, T. D., Folberth,
C., Frieler, K., Friend, A. D., Gerten, D., Gudmundsson, L., Hanasaki, N., Ito, A., Khabarov, N., Kim, H., Lawrence, P., Morfopoulos,
C., Müller, C., Müller Schmied, H., Orth, R., Ostberg, S., Pokhrel, Y., Pugh, T. A. M., Sakurai, G., Satoh, Y., Schmid, E., Stacke, T.,
30

Steenbeek, J., Steinkamp, J., Tang, Q., Tian, H., Tittensor, D. P., Volkholz, J., Wang, X., and Warszawski, L.: State-of-the-art global models underestimate impacts from climate extremes, *Nature Communications*, 10, 1005–, <https://doi.org/10.1038/s41467-019-08745-6>, 2019.

35

Stevanović, M., Popp, A., Lotze-Campen, H., Dietrich, J. P., Müller, C., Bonsch, M., Schmitz, C., Bodirsky, B. L., Humpenöder, F., and Weindl, I.: The impact of high-end climate change on agricultural welfare, *Science Advances*, 2, <https://doi.org/10.1126/sciadv.1501452>, <https://advances.sciencemag.org/content/2/8/e1501452>, 2016.

Taylor, K. E., Stouffer, R. J., and Meehl, G. A.: An Overview of CMIP5 and the Experiment Design, *Bulletin of the American Meteorological Society*, 93, 485–498, <https://doi.org/10.1175/BAMS-D-11-00094.1>, 2012.

Vadez, V., Berger, J. D., Warkentin, T., Asseng, S., Ratnakumar, P., Rao, K. P. C., Gaur, P. M., Munier-Jolain, N., Larmure, A., Voisin, A.-S., et al.: Adaptation of grain legumes to climate change: a review, *Agronomy for Sustainable Development*, 32, 31–44, 2012.

5 von Bloh, W., Schaphoff, S., Müller, C., Rolinski, S., Waha, K., and Zaehle, S.: Implementing the Nitrogen cycle into the dynamic global vegetation, hydrology and crop growth model LPJmL (version 5.0), *Geoscientific Model Development*, 11, 2789–2812, <https://doi.org/10.5194/gmd-11-2789-2018>, 2018.

Waha, K., Van Bussel, L., Müller, C., and Bondeau, A.: Climate-driven simulation of global crop sowing dates, *Global Ecology and Biogeography*, 21, 247–259, 2012.

10 Weedon, G. P., Balsamo, G., Bellouin, N., Gomes, S., Best, M. J., and Viterbo, P.: The WFDEI meteorological forcing data set: WATCH Forcing Data methodology applied to ERA-Interim reanalysis data, *Water Resources Research*, 50, 7505–7514, 2014.

Wheeler, T. and Von Braun, J.: Climate change impacts on global food security, *Science*, 341, 508–513, 2013.

White, J. W., Hoogenboom, G., Kimball, B. A., and Wall, G. W.: Methodologies for simulating impacts of climate change on crop production, *Field Crops Research*, 124, 357 – 368, <https://doi.org/10.1016/j.fcr.2011.07.001>, 2011.

15 Wiebe, K., Lotze-Campen, H., Sands, R., Tabeau, A., van der Mensbrugge, D., Biewald, A., Bodirsky, B., Islam, S., Kavallari, A., Mason-D'Croz, D., Müller, C., Popp, A., Robertson, R., Robinson, S., van Meijl, H., and Willenbockel, D.: Climate change impacts on agriculture in 2050 under a range of plausible socioeconomic and emissions scenarios, *Environmental Research Letters*, 10, 085010, <https://doi.org/10.1088/1748-9326/10/8/085010>, <https://doi.org/10.1088%2F1748-9326%2F10%2F8%2F085010>, 2015.

20 Williams, K., Gornall, J., Harper, A., Wiltshire, A., Hemming, D., Quaife, T., Arkebauer, T., and Scoby, D.: Evaluation of JULES-crop performance against site observations of irrigated maize from Mead, Nebraska, *Geoscientific Model Development*, 10, 1291–1320, <https://doi.org/10.5194/gmd-10-1291-2017>, 2017.

Williams, K. E. and Falloon, P. D.: Sources of interannual yield variability in JULES-crop and implications for forcing with seasonal weather forecasts, *Geoscientific Model Development*, 8, 3987–3997, <https://doi.org/10.5194/gmd-8-3987-2015>, 2015.

25 Wolf, J. and Oijen, M.: Modelling the dependence of European potato yields on changes in climate and CO₂, *Agricultural and Forest Meteorology*, 112, 217 – 231, [https://doi.org/10.1016/S0168-1923\(02\)00061-8](https://doi.org/10.1016/S0168-1923(02)00061-8), 2002.

Wu, X., Vuichard, N., Ciais, P., Viovy, N., de Noblet-Ducoudré, N., Wang, X., Magliulo, V., Wattenbach, M., Vitale, L., Di Tommasi, P., Moors, E. J., Jans, W., Elbers, J., Ceschia, E., Tallec, T., Bernhofer, C., Grünwald, T., Moureaux, C., Manise, T., Ligne, A., Cellier, P., Loubet, B., Larmanou, E., and Ripoche, D.: ORCHIDEE-CROP (v0), a new process-based agro-land surface model: model description and evaluation over Europe, *Geoscientific Model Development*, 9, 857–873, <https://doi.org/10.5194/gmd-9-857-2016>, 2016.